

A NEW MULTI-OUTPUT DC-DC CONVERTER FOR USE WITH ELECTRIC VEHICLES

1. THOMALA PRIYANKA, 2. YETHIRAJULA KISHORE, 3. NYDHANA SAI, 4. PARRE ARUN
5. YARRAMSETTI PURNA CHANDRA TEJA, 6*U. LAKSHMI, ASSISTANT PROFESSOR,

DEPARTMENT OF ELECTRICAL AND ELETRONICS ENGINEERING

SANKETIKA VIDYA PARISHAD ENGINEERING COLLEGE, VISAKHAPATNAM

ABSTRACT: - The use of multiport converters in portable electronics and electric vehicles (EV) is important. Different single-input multi-output (SIMO) converter configurations are presented in the literature. Most SIMO converters provide outputs with duty ratio operational restrictions. As well as inductors' charging. Designing SIMO converters still faces the challenge of the cross-regulation issue. In this work, a SIMO architecture is suggested to get beyond the earlier described restrictions. It can produce three alternative output voltages (such as $iL1 > iL2 > iL3$ or $iL1 \ iL2 \ iL3$) without being constrained by the duty cycle or inductor currents. The proposed topology does not have cross regulation issues, hence changes in output current $iO3$ ($iO2$) ($iO1$) have no effect on the load voltage $V01$ ($V02$) ($V03$). During control, the loads are separated from one another. A 200 W prototype circuit is created in the lab, and the findings of simulation and testing are confirmed.

INDEX TERMS: - Multiport converters, single input multi output converters.

I. INTRODUCTION

The use of renewable energy sources in electric vehicles (EVs), auxiliary power, and grid-connected applications has seen a growth in demand over the last ten years [1]– [5]. Multiport DC-DC converters are crucial in these applications because they enable the hybridization of energy sources, which lowers the system's component count, complexity, and cost as compared to many separate single input DC-DC converters [6], [7].

MPC converters have been made available throughout the previous ten years. In [8], a brand-new SIMO converter is suggested. This structure produces independent boost, buck, and inverted outputs all at once. However, providing 'n' voltage levels necessitates n^2 switches, increasing the converter's overall size and price. Unexpected errors in the computation of the output voltages and state-space equations for a SIMO converter are addressed and corrected in [9]. In comparison to single inductor SIMO converters, the single coupled inductor-based SIMO buck is shown in [10] to have smaller output inductor current ripple. In depth comparisons of the cross-coupling performance of SIDO converters based on coupled inductor and single inductor (SI) were reported by Nayak and Nath [11]. They also suggested that the coupled inductor SIDO converter performs better in steady-state and transient situations. However, a SI SIMO setup switches the inductor between the loads, resulting in large ripples and cross-regulation issues.

To solve the cross-regulation problem in a single inductor-based SIMO converter, various control strategies are put forth in the literature; the current predictor controller is described in [12] as an alternative to the traditional charge balance strategy. However, it has been challenging to generate the duty ratios for active switches. Like this, [13] presents the deadbeat-based control technique. Because it is dependent on an output current observer, it is susceptible to noise and severe parametric changes. To reduce voltage ripples, eliminate cross-regulation issues, and manage output voltages, a multivariable digital controller-based

SIMO converter is suggested in [14]. However, complexity may rise as a result of controller design.

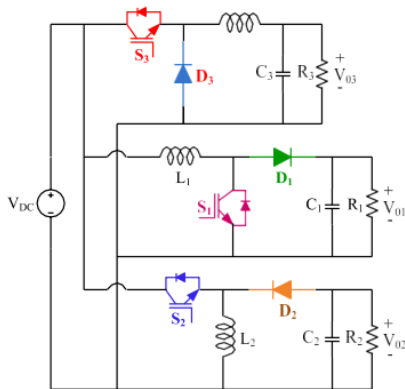


FIGURE 1. Diagram of conventional SIMO converter.

[15] presents a non-isolated, single-switch SIMO converter topology. It lowers the system's cost and has fewer components. Nevertheless, it might be difficult to separately control the outputs.

A non-isolated SIMO converter is suggested in [16]–[25] to address the issues with a single inductor SIMO converter. This converter has independently regulated output voltages and does not need an additional control circuit. For generating the step-up and step-down output voltages for electrical vehicle applications, a new SIDO converter topology is described in [16] that integrates buck and super lift converter. It features a limitation called D2 D1, which reduces D1's operational range by raising D2. Less semiconductor switches are used in the topologies suggested in [17] and [18]. But the converter's operation depends on how quickly inductors charge (i.e., $iL1 > iL2$). So, the restriction on the on-duty ratio is maintained.

For PV applications, [19] suggests combining high gain step-up with SEPIC converter-based SIMO. The capacitors and diodes increase the output voltage in this setup such that both outputs are higher than the supply voltage. Nevertheless, cost and conduction losses are influenced by the quantity of capacitors and diodes. In [20], a brand-new SIDO buck-boost topology is created to produce both positive and negative outputs. [21] suggests of a multi-output converter with a smaller part count. But because there are more diodes, there are more conduction losses. In [22], a construction with a SIMO design is introduced, having the benefits of a smaller passive filter and lower

voltage stress. Based on the front-end switched-capacitor approach, a high-density multi-output converter is described in [23] for portable electronic applications with enhanced power density and decreased switching losses.

In [24], a modified SEPIC and an interleaved-based high step-up SIMO converter are presented. It has a voltage multiplier, connected inductor, and switching capacitors to increase the output voltage in applications for sustainable energy. Due to the increased number of components, it is complicated. For SIMO applications, the SEPIC-Cuk converter-based four-phase interleaved converter is recommended in [25]. It benefits from low ripple voltage, compact size, and high-power applications compatibility with dynamic response.

In the traditional method, Figure 1 depicts the auxiliary power supply system for EVs to fulfil the load needs. Although it appears straightforward, this method has a cross-regulation issue, and the loads are not isolated from one another while they are operating. Additionally, there is a possibility of grounding problems when the battery is being charged and many loads are turned on at the same time. To bring one of the negative output voltages into buck-boost operation mode, the circuit complexity will also rise.

The onboard power converter is the primary focus of the planned development. The circuit in Figure 2(a) is set up so that energy stored in the inductor is restricted to only one output and is not shared with the other outputs during control, allowing the output voltages to be regulated with independent duty cycles. More crucially, the loads are kept apart throughout control, which effectively solves the cross-regulation issue. Additionally, even if battery charging and grounding are involved, there are no issues with grounding because there is an onboard power converter.

The remainder of the article is divided into the following sections: Section II presents the developed SIMO configuration and modes of operation. Section III presents small-signal modelling. Section IV discusses the controller design, parameter design, power loss analysis, and comparative evaluation. Section V displays the simulation, experiment, and results. Section VI contains a summary.

II. PROPOSED SIMO CONFIGURATION AND MODES OF OPERATION

Figure 2(a) shows the suggested single input, three output DC-DC design. The following components make up this configuration: input voltage VDC, switches S1–S3, diodes D1–D3, and passive components L1–C1, L2–C2, and L3–C3. It can produce boost (V01), buck-boost (V02) with positive voltage polarity, and buck (V03), three separate output voltages. With the duty cycles D1, D2, and D3, the suggested converter can independently control the output voltages. Figure 2(b) shows the theoretical waveforms of circuit components.

Contrary to the usual parallel configuration of buck, boost, and buck-boost, the proposed configuration is unusual. The loads are isolated during the simultaneous control in the suggested circuit arrangement. The loads R3 and S3 alone are connected to the input power supply during mode-1 operation, as indicated in the following images, but the other loads are separated, as shown in Figure 3(a). Like mode 1, mode 2 isolates all other loads and solely connects load R1 through D1 to the input supply, as shown in Figure 3(b). In the suggested control technique, all loads are kept apart while being controlled in any mode of operation. But this function is not possible.

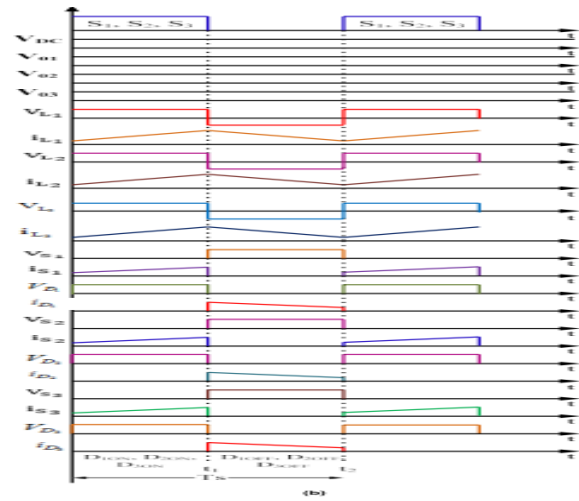
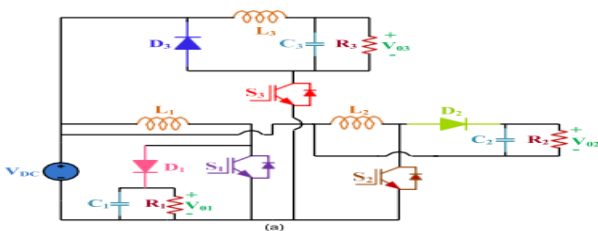


FIGURE 2. Proposed configuration: (a) SIMO configuration, (b) Theoretical waveforms.

converters that use buck, boost, and buck-boost operation in simultaneously. This circuit arrangement appears to be quite straightforward, however it is unique and useful. Table 1 below compares the traditional and suggested SIMO converters in terms of the quantity of components, modes of operation, and working circumstances.

TABLE 1. Parameter specification comparison between the conventional and proposed SIMO converter.

Comparison different aspects	Conventional	Proposed
Number of components	6	6
Output voltage	Buck, Boost, and Buck-Boost (Negative output voltage)	Buck, Boost, and Buck-Boost (Positive output voltage)
Inverting circuit is required for the positive output voltage	Yes	No
Loads are isolated to each other during control	No	Yes

The cross-regulation issue and the lack of load isolation during operation are the key drawbacks of the typical technique depicted in Figure 1. In the buck-boost mode of operation, the circuit complexity will also rise in order to convert the negative polarity of output voltages.

The following benefits of the suggested structure:

- a) The construction is straightforward, with no operating duty ratio assumptions ($D1 > D2 > D3$ or $D3 > D2 > D1$ or $D1 > D2 > D3$) =
- b) It can produce boost, buck, and buck-boost output voltages, respectively
- c) There are no restrictions on inductor currents (such as $iL1 > iL2 > iL3$, $iL1 > iL2 > iL3$, or $iL1 > iL2 > iL3$).
- d) During control, loads are kept apart from one another, and the cross-regulation issue is successfully fixed.
- e) It gives the positive buck-boost output voltage

A. MODES OF OPERATION

1) SWITCHING STATE 1

S1, S2, and S3 switches are all turned on. Figure 3(a) shows the current flow path, and the energy port VDC magnetises L1, L2, and L3. In light of this, the C1 and C2 are discharged to the corresponding loads (R1) and (R2), whereas (C3) is charged. Eq. (1)–(4) represents the capacitor voltages and inductor currents.

$$i_{L1}(t) = \frac{V_{DC}}{L1}t + i_{L1(0)} \quad v_{C1}(t) = v_{C1(0)}e^{-\frac{t}{R1C1}} \quad (1)$$

$$i_{L2}(t) = \frac{V_{DC}}{L2}t + i_{L2(0)} \quad v_{C2}(t) = v_{C2(0)}e^{-\frac{t}{R2C2}} \quad (2)$$

$$i_{L3}(t) = \frac{V_{DC}}{L3} + e^{-\alpha t} [c1 \cos \omega_d t + c2 \sin \omega_d t] \quad (3)$$

$$v_{C3}(t) = V_{DC} - \frac{1}{2C3} e^{-\alpha t} \left[\cos \omega_d t \left(\frac{\alpha C1}{R} + \omega_d c2 \right) + \sin \omega_d t \left(-\alpha c2 + \frac{\omega_d c1}{R3} \right) \right] \quad (4)$$

2) SWITCHING STATE 2

In this condition, L1, L2, and L3 are demagnetized and, through D1, D2, and D3, respectively, supply their energy to the load.

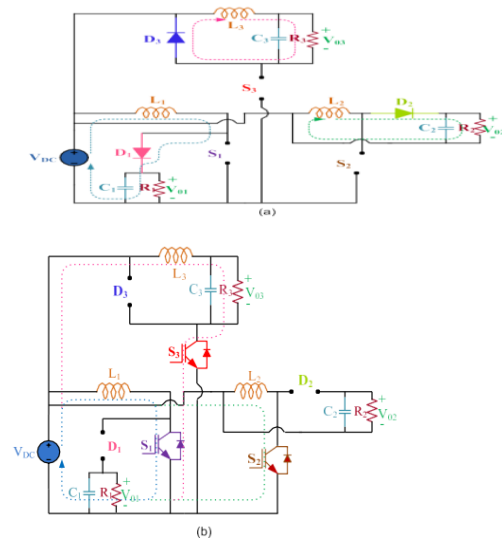


FIGURE 3. Operating states: (a) Switching state-1 and (b) Switching state-2.

Figure 3(b) provides an example of it. Eq. (5)–(11) shows the following capacitor voltages and inductor currents:

$$i_{L1}(t) = \frac{V_{DC}}{R1} + e^{-\alpha t} [c1 \cos \omega_{d1} t + c2 \sin \omega_{d1} t] \quad (5)$$

$$v_{C1}(t) = V_{DC} - \frac{1}{2C1} e^{-\alpha t} \left[\cos \omega_{d1} t \left(\frac{\alpha C1}{R1} - \omega_{d1} c2 \right) + \sin \omega_{d1} t \left(\omega_{d1} c1 + \frac{c2}{R1} \right) \right] \quad (6)$$

$$i_{L2}(t) = e^{-\alpha t} [c3 \cos \omega_{d2} t + c4 \sin \omega_{d2} t] \quad (7)$$

$$v_{C2}(t) = -L2 e^{-\alpha t} \left[(-\alpha c3 + \omega_{d2} c4) \cos \omega_{d2} t + \dots \right] \quad (8)$$

$$i_{L3}(t) = e^{-\alpha t} [c5 \cos \omega_{d3} t + c6 \sin \omega_{d3} t] \quad (9)$$

$$v_{C3}(t) = -L3 e^{-\alpha t} \left[(-\alpha c5 + \omega_{d3} c6) \cos \omega_{d3} t + (\omega_{d3} c5 + \frac{\alpha c6}{R3}) \sin \omega_{d3} t \right] \quad (10)$$

$$\alpha_1 = \frac{2R1C1}{L1}, \quad \omega_{d1} = \frac{1}{L1C1} \sqrt{1 - \frac{R1^2 C1^2}{4L1^2}}$$

$$\alpha_2 = \frac{2R2C2}{L2}, \quad \omega_{d2} = \frac{1}{L2C2} \sqrt{1 - \frac{R2^2 C2^2}{4L2^2}}$$

$$a = \frac{1}{2R_3C_3}, \quad \omega_d = \frac{1}{2} \sqrt{\frac{1}{R_3^2C_3^2} - \frac{4}{L_3C_3}}, \quad (11)$$

where the initial values for c1, c2, c3, c4, c5, and c6.

The suggested configuration's output voltages are as follows.

$$V_{01} = \frac{V_{DC}}{(1 - D_1)}, \quad V_{02} = \frac{V_{DC}D_2}{(1 - D_2)}, \quad V_{03} = D_3V_{DC} \quad (12)$$

Duty ratios for the S1, S2, and S3 are D1, D2, and D3, respectively.

While the other loads are segregated even when the ground is involved when charging the battery, it is noticeable that load (R3) alone through S4 is linked to the ground when switching state-1 operation, as illustrated in Figure 3(a). Like switching state 1, only load (R1) linked to the ground through D1 during switching state 2 isolates all other loads from the ground and load (R1), as seen in Figure 3(b). In the suggested control technique, all loads are kept apart while being controlled in any mode of operation. Additionally, the circuit is set up so that energy from the inductor is restricted to only one output during control and is not shared with the other outputs. This setup also enables managing the output voltages with independent duty cycles. As a result, the fluctuation in load current (i03, i02, and i01) has no effect on the load voltage (V01, V02, and V03). Therefore, even when the ground is engaged during battery charging, the suggested arrangement with this control approach eliminates all the issues of cross regulation problems. The arrangement is straightforward and can produce three distinct outputs without making any assumptions about the inductor currents (iL1 > iL2 > iL3 or iL1 iL2 iL3) and/or operating duty cycle.

B. SEMICONDUCTOR STRESS ANALYSIS

Eqs (13)– (15) present the proposed configuration's semiconductor stresses as [27].

1) VOLTAGE STRESSES

$$V_{S1} = V_{01}, \quad V_{D1} = V_{01}, \quad V_{S2} = V_{02} + V_{DC}, \quad V_{D2} = (V_{02} + V_{DC}) = V_{02} = V_{DC}^2 \quad (13)$$

2) CURRENT STRESSES

A: MODE 1

$$i_{S1} = i_{L1}, \quad i_{D1} = 0, \quad i_{S2} = i_{L2}, \quad i_{D2} = 0, \quad i_{S3} = i_{L3}, \quad i_{D3} = 0 \quad (14)$$

b: MODE 2

$$i_{S1} = i_{D1} = i_{L1}, \quad i_{S2} = i_{S3} = 0, \quad i_{D2} = i_{L1}, \quad i_{D3} = i_{L3} \quad (15)$$

TABLE 2. Parameter specifications.

Parameter	Simulation	Experimental
Input voltage (V _{in})	50 V	50 V
Output voltage (V _{o1} /V _{o2} /V _{o3})	100/50/25 V	100/50/25 V
Output currents (I _{o1} /I _{o2} /I _{o3})	2/2/2 A	2/2/2 A
Switching frequency (f)	50 kHz	50 kHz
Inductor (L ₁ /L ₂ /L ₃)	0.6/0.9/1 mH	0.5/1/1 mH
Capacitor (C ₁ /C ₂ /C ₃)	200/470/360 uF	220/470/470 uF

V. RESULTS AND DISCUSSIONS

A. SIMULATION RESULTS

The model was created in the MATLAB environment to validate the suggested system using 50 V DC, 50 kHz frequency, and a 50% duty ratio. The parameter information is TABLE 3. Comparison between different SIMO topologies.

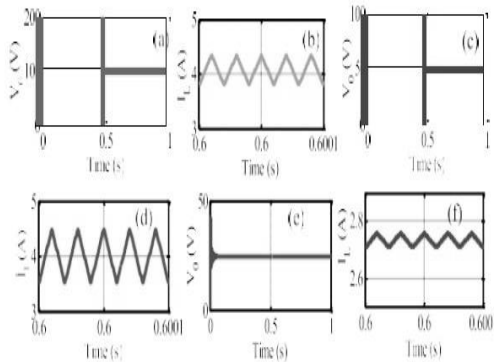


Fig4

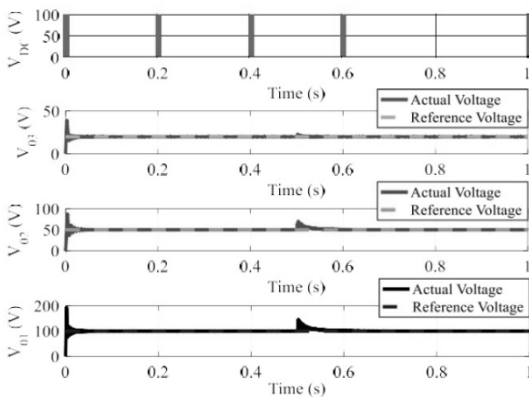


Fig 5

Figure 4(a-f) shows the matching output voltages (V_{01} , V_{02} , and V_{03}) and inductor currents (i_{L1} , i_{L2} , and i_{L3}). These values are stated in Table 2. The output voltages shown in Figures 4(a), 4(c), and 4(e) are nearly identical to the predicted values. For the suggested setup, closed-loop control is put into practise, and the total system's dynamic performance is tested for a sudden change in input voltage. The simulation output for closed-loop control is shown in Figure 5 for an abrupt shift in input voltage (VDC) from 50 V to 70 V at 0.5 sec. For the Buck output, the PI control gains are $K_p = 0.1$ and $K_i = 15$, whereas for the Boost and Buck-Boost voltages, $K_p = 0.005$ and $K_i = 0.5$.

TABLE 3. Comparison of complexity, power density, and efficiency.

Ref.	Complexity		Power density	
	Power switches	Complexity in controller design	Total number of components	Power density In each topology
20	S=2	Less	10	High
19	S=1	Less	24	Low
18	S=3	Less	7	High
21	S=2	Less	18	Low
22	S=4	Less	11	High
23	S=12	High	23	Low
Proposed	S=2	Less	12	High

The findings demonstrate that the suggested arrangement produces rigid independent output voltages and is unaffected by a sudden change in supply.

VI. CONCLUSION

This paper suggests the SIMO converter's structure. The operational theory and modes of operation have been thoroughly explained. The suggested arrangement is straightforward and makes no assumptions on the inductors' charging or operating duty cycle. With independent regulated voltages, it can produce the output voltages for buck, boost, and buck-boost. Since there are no cross-regulation issues in the suggested design, the quick change in inductor and load currents has no impact on the output voltages. Finally, simulation and experiment findings support the performance and operation of the suggested converter.

REFERENCES

[1] P. C. Heirs, Z. Saadat Zadeh, and E. Babaei, "A newton input-single output high voltage gain converter with ripple-free input currents and reduced voltage on semiconductors," *IEEE Trans. Power Electron.*, vol. 34, no. 8, pp. 7693–7702, Aug. 2019, Doi: 10.1109/TPEL.2018.2880493.

[2] A. Fara Khor, M. Aba pour, and M. Sabahi, "Design, analysis, and implementation of a multiport DC–DC converter for renewable energy applications," *IET Power Electron.*, vol. 12, no. 3, pp. 465–475, Mar. 2019.

[3] S. K. Mishra, K. K. Nayak, M. S. Rana, and V. Dharmaraja, "Switched boost action based multiport converter," *IEEE Trans. Ind. Appl.*, vol. 55, no. 1, pp. 964–975, Jan./Feb. 2019.

- [4] X. Lu, K. L. V. Iyer, C. Lai, K. Mukherjee, and N. C. Kar, "Design and testing of a multi-port sustainable DC fast-charging system for electric vehicles," *Electra. Power Compony. Syst.*, vol. 44, no. 14, pp. 1576–1587, Aug. 2016.
- [5] E. Babaei and O. Abbasi, "A new topology for bidirectional multi-input multi-output buck direct current–direct current converter," *Int. Trans. Electra. Energy. Syst.*, vol. 27, no. 2, pp. 1–15, Feb. 2017.
- [6] Z. Rehman, I. Al-Badly, and S. Mukhopadhyay, "Multiplug DC–DC converters in renewable energy applications—An overview," *Renew. Sustain. Energy Rev.*, vol. 41, pp. 521–539, Jan. 2015.
- [7] G. Chen, Y. Liu, X. Qing, and F. Wang, "Synthesis of integrated multi-port DC–DC converters with reduced switches," *IEEE Trans. Ind. Electron.*, vol. 67, no. 6, pp. 4536–4546, Jun. 2019.
- [8] P. Patra, A. Patra, and N. Misra, "A single-inductor multiple-output switcher with simultaneous buck, boost, and inverted outputs," *IEEE Trans. Power Electron.*, vol. 27, no. 4, pp. 1936–1951, Apr. 2012.
- [9] M. Abbasi, A. Afifi, and M. R. A. Pahlavi, "Comments on 'a singleinductor multiple-output switcher with simultaneous buck, boost, and inverted outputs,'" *IEEE Trans. Power Electron.*, vol. 34, no. 2, pp. 1980–1984, Feb. 2019.
- [10] Y.-C. Hsu, J.-Y. Lin, C.-H. Wang, and S.-W. Chou, "A SIMO step down converter with coupled inductor," in *Proc. Int. Symp. VLSI Design, Autom. Test (VLSI-DAT)*, Hsinchu, Taiwan, Aug. 2020, pp. 1–4, Doi: 10.1109/VLSI-DAT49148.2020.9196435.
- [11] G. Nayak and S. Nath, "Comparing performances of SIDO buck converters," in *Proc. IEEE Int. Conf. Power Electron., Drives Energy Syst. (PEDES)*, Chennai, India, Dec. 2018, pp. 1–6.
- [12] Y. Zheng, J. Guo, and K. N. Leung, "A single-inductor multiple-output buck/boost DC–DC converter with duty-cycle and control-current predictor," *IEEE Trans. Power Electron.*, vol. 35, no. 11, pp. 12022–12039, Nov. 2020.
- [13] X. Zhang, B. Wang, X. Tan, H. B. Goo, H. H.-C. Io, and T. Fernando, "Deadbeat control for single-inductor multiple-output DC–DC converter with effectively reduced cross regulation," *IEEE J. Emerg. Sel. Topics Power Electron.*, vol. 8, no. 4, pp. 3372–3381, Dec. 2020.
- [14] J. D. Dasia, B. Bahrani, M. Seedfield, A. Karimi, and A. Rufer, "Multivariable control of single-inductor dual-output buck converters," *IEEE Trans. Power Electron.*, vol. 29, no. 4, pp. 2061–2070, Apr. 2014.
- [15] E. Durán, S. P. Libran, and M. B. Ferrera, "Configurations of DC–DC converters of one input and multiple outputs without transformer," *IET Power Electron.*, vol. 13, no. 12, pp. 2658–2670, Sep. 2020.
- [16] B. Farida, M. Farrokh far, M. Nasiri, A. Kalahari, and N. Seadog, "Developing a super-lift Luo-converter with integration of buck converters for electric vehicle applications," *CSEE J. Power Energy Syst.*, vol. 7, no. 4, pp. 811–820, Jul. 2021, Doi: 10.17775/CSEEJPES.2020.01880.
- [17] O. Ray, A. Josyula, S. Mishra, and A. Joshi, "Integrated dual-output converter," *IEEE Trans. Ind. Electron.*, vol. 62, no. 1, pp. 371–382, Jan. 2015.
- [18] G. Chen, Y. Deng, J. Dong, Y. Hu, L. Jiang, and X. He, "Integrated multiple-output synchronous buck converter for electric vehicle power supply," *IEEE Trans. Veh. Technol.*, vol. 66, no. 7, pp. 5752–5761, Jul. 2017.
- [19] M. S. B. Ranjana, N. S. Reddy, and R. K. P. Kumar, "A novel septic based dual output DC-DC converter for solar applications," in *Proc. Power Energy Syst., Towards Sustain. Energy*, Mar. 2014, pp. 1–5.

- [20] J. Marjani, A. Imani, E. Adjei, and A. Hekmati, "A new dual output DC-DC converter with enhancing output voltage level," in Proc. 24th Iranian Conf. Electra. Eng. (ICEE), May 2016, pp. 573–577.
- [21] Z. Saadat Zadeh, P. C. Heirs, E. Babaei, and M. Sabahi, "A new no isolated single-input three-output high voltage gain converter with low voltage stresses on switches and diodes," IEEE Trans. Ind. Electron., vol. 66, no. 6, pp. 4308–4318, Jun. 2019.
- [22] A. Ganj Avi, H. Ghomeshi, and A. A. Ahmad, "A novel single-input dual output three-level DC-DC converter," IEEE Trans. Ind. Electron., vol. 65, no. 10, pp. 8101–8111, Oct. 2018.
- [23] S. M. Haussamen, A. Parodic, and D. A. Johns, "An integrated high density power management solution for portable applications based on a multioutput switched-capacitor circuit," IEEE Trans. Power Electron., vol. 31, no. 6, pp. 4305–4323, Jun. 2016.
- [24] M. Y. Hassani, M. Malanda's, and S. H. Hosseini, "A new single input multioutput interleaved high step-up DC-DC converter for sustainable energy applications," IEEE Trans. Power Electron., vol. 36, no. 2, pp. 1544–1552, Feb. 2021.
- [25] E. D. Aranda, S. P. Libran, and M. B. F. Prieto, "An interleaved single input multiple-output DC-DC converter combination," CSEE J. Power Energy Syst., vol. 8, no. 1, pp. 132–142, Jan. 2022, Doi: 10.17775/CSEEJPES.2020.00300.
- [26] V. Rama Narayanan, Course Material on Switched Mode Power Conversion. Bangalore, India: IISc., Jan. 2008.
- [27] M. K. Kazimierz, Pulse-Width Modulated DC-DC Power Converters, 1st ed. Hoboken, NJ, USA: Wiley, 2008.
- [28] R. S. Alishah, D. Azimpour, S. H. Hosseini, and M. Sabahi, "Reduction of power electronic elements in multilevel converters using a new cascade structure," IEEE Trans. Ind. Electron., vol. 62, no. 1, pp. 256–269, Jan. 2015.
- vol. 65, no. 6, pp. 4810–4818, Jun. 2018.